

# A WIND-TUNNEL FACILITY FOR SIMULATING MOUNTAIN AND HEATED-ISLAND GRAVITY WAVES

TETSUJI YAMADA\* and ROBERT N. MERONEY\*\*

*Fluid Mechanics Program, Dept. of Civil Engineering, Colorado State University,  
Fort Collins, Colo. 80521, U.S.A.*

(Received in final form 24 September, 1973)

**Abstract.** A wind tunnel was constructed to study mountain lee-wave phenomena and heated-island effects. The present wind tunnel appears to have several advantages over a towing tank facility for modeling atmospheric gravity-wave phenomena, i.e., non-uniform approach flows, stationary measuring conditions, variation of boundary temperature condition in the longitudinal direction, and no slip at the wall. Simple design criteria and characteristics of the present wind tunnel are discussed. A numerical program was utilized to explain peculiar standing-wave disturbances in the wind-tunnel test section. The above disturbances seemed unavoidable under the chosen mechanical constants. Nevertheless, a practical solution was found by extending the tunnel length.

## 1. Introduction

This paper reports the design and characteristics of a laboratory technique to simulate some aspects of geophysical stratified flow fields. Internal gravity-wave motions have been studied by all available means: analytically, experimentally by field and model studies and by the use of large computers. Yet, although much light has been shed on the question, the results are still only fragmentary, for the problem is complex – and all approaches have inherent limitations. In particular, there is a need for detailed flow field measurements against which to test analytical and numerical models – even if all aspects of the full-scale geophysical situations are not present.

Field studies of atmospheric internal gravity waves are very expensive on the large scale required; therefore, they have not been exhaustive. Despite this restriction on prototype measurements, only a limited laboratory simulation of mountain lee waves has been attempted. No laboratory simulation of the heat-mountain phenomenon is known to the authors. Abe (1932) investigated the formation of mountain clouds over Mount Fuji, which is an almost conical mountain. In his experiments, a model geometrically similar to Mount Fuji, scaled in the ratio 1:50000, was used. The experiments were conducted in a wind tunnel at the same Reynolds number under the assumption that molecular viscosity in the laboratory corresponded to eddy viscosity in the atmosphere. An attempt was made to introduce temperature stratification, but the Froude number was not consistent between model and prototype flows.

Long (1955), Suzuki and Yabuki (1956), and Davis (1969) conducted simulation experiments with water in which the density stratification was obtained by additions of salt or a brine. In order to avoid turbulent mixing of the fluid, they kept the liquid

\* Postdoctoral Fellow, Princeton University, New Jersey, U.S.A.

\*\* Associate Professor, Fluid Mechanics Program, Colorado State University, Fort Collins, U.S.A.

stationary and moved the barrier through it. Long (1959) conducted simulation experiments of flows over the Sierra Nevada with remarkable correlation. These towing tank experiments were of course limited to uniform approach flows. The resulting slip condition at the boundary appears unrealistic.

The seemingly obvious choice of a stratified wind tunnel for laboratory simulation has been forestalled by the large temperature gradients and low velocities required for simulation. In order to simulate atmospheric gravity waves or thermal plume behavior in the laboratory, the modeling apparatus must possess the capability of introducing enough stratification in the fluid to reproduce a ratio of inertial to gravity forces – embodied in the Froude number – of the same order of magnitude as occurs in the natural atmosphere. The effects of fluid properties, Prandtl number, and other dynamic force fields, Reynolds number, must also be considered. Finally, a similarity in boundary conditions must be satisfied. Queney (1960) in particular, doubted that a laboratory model, particularly in a wind tunnel, could reproduce the essential characteristics of the atmosphere in the planetary boundary layer. A typical model experiment would require a flow speed of the order of  $5\text{--}10\text{ cm s}^{-1}$  and a temperature gradient of  $1\text{--}2^\circ\text{C cm}^{-1}$ . Queney concludes,

... Such flows with large temperature gradients and very low flow speeds *cannot be accomplished*, at least in conventional wind tunnels. Furthermore at such low velocities (small Reynolds number) considerable boundary-layer effects would arise near the tunnel walls, and the assumption of no friction would be invalidated. The above considerations indicate that model experiments in wind tunnels using air as the streaming medium would be *useless* if it is desired to accomplish quantitative similarity...\*

Recent experiments of free shear flows and plume dispersion in small stratified wind tunnels reveal that large standing wave systems tend to appear just downstream of the tunnel entrance (Scotti, 1969; Hewett *et al.*, 1970; Corcos and Sherman, 1970). Scotti, Corcos, and Sherman attribute the undesirable standing waves to the effect of wall contraction for a fluid system where the duct Froude number is less than 1. (They argue one must avoid situations in which  $F_1^2 + F_2^2 < 1$ , where  $F_1^2$  and  $F_2^2$  are local densimetric Froude numbers ( $F^2 = \rho v^2 / g \Delta \rho d$ ) of adjacent layers.) Hewett *et al.* (1970) commented upon the presence of stagnant layers of fluid and standing internal waves in terms of the experience of Yih (1965) with two-dimensional sink flows in stratified fluids. Yih predicted anomalous behavior in stratified channel flow for  $Fr_D < 1/\pi$ . In order to minimize heat transfer through the wind-tunnel side walls, the average temperature inside the tunnel was kept close to room temperature. The authors believed that this temperature distribution arrangement resulted in two natural convection cells which blocked the tunnel stream and induced waves. Hence, Hewett *et al.* (1970) concluded that their tunnel was not suitable for modeling atmospheric phenomena for  $Fr_D < 1/\pi$ .

Despite the difficulties outlined above, it was concluded that the advantages of improved boundary conditions, the prospect of non-uniform velocity fields, and a

\* Italics for emphasis.



greater potential for detailed measurements of the temperature and velocity fields justified the design and construction of a stratified air flow facility. The results suggest earlier investigations were overly pessimistic in their estimates of the potential for wind-tunnel laboratory studies.

## 2. Simulation Criteria

*Similarity in mountain lee-wave phenomena* – The complete similarity requirements for a mountain lee-wave phenomenon were described by Lin and Binder (1967) who considered the effect of Reynolds number in detail and concluded that vertical velocities associated with boundary-layer growth are three orders of magnitude smaller than vertical velocities associated with mountain waves. Here only certain aspects of geometric and dynamic similarity will be discussed.

Following the arguments in Queney (1960, p. 104), the Scorer function is given as

$$S_c = M^2 \left( \frac{sg}{\bar{u}^2} - \frac{(\partial^2 \bar{u} / \partial z^2)}{\bar{u}} \right).$$

If the shear term is neglected, then the Scorer function may be interpreted as an overall Richardson number based on the mountain height,  $M$ . If the following values are substituted (obtained from a typical mountain lee-wave situation):

$$\gamma = 0.006^\circ\text{C m}^{-1}$$

$$\bar{T} = 250 \text{ K},$$

$$\bar{u} = 20 \text{ m s}^{-1},$$

then

$$s = 1.6 \times 10^{-5} \text{ m}^{-1} \quad \text{and} \quad sg/\bar{u}^2 = 0.4 \text{ km}^{-2} \quad \text{for the atmosphere.}$$

If a geometric scaling is 1 to 30000 and the temperature gradient in a wind tunnel can be maintained at  $1^\circ\text{C cm}^{-1}$ , the velocity in a model experiment must be  $8.6 \text{ cm s}^{-1}$  for dynamic similarity.

*Similarity in heated island phenomena* – According to a linearized theory proposed by Stern and Malkus (1953), it is necessary to satisfy  $\sqrt{gs} k/U^2 > \frac{1}{2}$  in order to simulate an equivalent mountain capable of developing strong gravity waves downwind of a heated boundary. It will be easily seen that the above relation, because it requires an unusually large stability and a small velocity, cannot be satisfied in any existing wind-tunnel facility. For example,  $s = 3 \times 10^{-3} \text{ cm}^{-1}$  ( $\partial T/\partial z \approx 1^\circ\text{C cm}^{-1}$ ) and  $k = 0.2 \text{ cm}^2 \text{ s}^{-1}$  requires  $u < 0.83 \text{ cm s}^{-1}$ . If  $u = 4 \text{ cm s}^{-1}$  and  $k = 0.2 \text{ cm}^2 \text{ s}^{-1}$ , then  $s > 2.63 \text{ cm}^{-1}$  is required for a simulation, which is equivalent to  $500^\circ\text{C cm}^{-1}$ . Thus for reasonable temperature gradients, it is impossible to satisfy the relation  $\sqrt{gs} k/U^2 > \frac{1}{2}$  unless viscosity  $k$  is artificially modified by a factor of at least 30. Thus a thermal equivalent mountain in a wind-tunnel experiment must take a plateau shape: the mountain starts at the leading edge of the island and increases asymptotically to reach its maximum height directly above the end of the island, then decreases exponentially.

To see the shape of a thermal mountain which might be simulated, the following numerical values are substituted into the linear theory of Stern and Malkus:

$$k = 0.2 \text{ cm}^2 \text{ s}^{-1}$$

$$\Delta L = \text{island width} = 8 \text{ cm}$$

$$u = 4 \text{ cm s}^{-1}$$

$$s = 4.67 \times 10^{-3} \text{ cm}^{-1} \quad (\partial T / \partial z = 1.4^\circ \text{C cm}^{-1}, \bar{T} = 300 \text{ K})$$

$$\Delta T = \text{temperature excess} = 56^\circ \text{C}.$$

The computed mountain profile increases in height almost linearly to 8.4 cm at the end of the island, then decreases exponentially, taking the values of 6.1, 2.3, and 0.1 cm at  $x = 30, 100,$  and  $350 \text{ cm}$ , respectively.

Summarizing, it evidently is necessary to obtain a velocity ranging from 4 to 15  $\text{cm s}^{-1}$ , and a temperature gradient of  $0.5^\circ \text{C cm}^{-1}$  to  $1.5^\circ \text{C cm}^{-1}$ , in order to simulate atmospheric lee-wave phenomena and heated island problems in a wind-tunnel facility. No Prandtl number restriction is present since equivalent fluids are utilized in the prototype and laboratory flow fields. The above requirements are equivalent to attaining a Froude number based on the wind-tunnel height (60 cm) from 0.030 to 0.196.

### 3. The Experimental Facility

Although there are quite a few low-speed, small wind tunnels (Pope and Hooper, 1966), guidance for the design of a thermal wind tunnel is limited. Several reports are available, including Plate and Cermak (1963), Webster (1964), Strom and Kaplin (1968), Charpentier (1967), Scotti (1969), and Hewett *et al.* (1970). Each of these facilities was designed to satisfy special purposes, and duplication of their designs did not appear desirable. The tunnels of Strom and Kaplin, and Charpentier could not produce the strong temperature gradient required here; Scotti was primarily interested in a free shear layer whose thickness was about 6 mm; and the facility of Hewett *et al.* (1970) was suitable for flows whose duct Froude numbers were greater than  $1/\pi$ .

Nevertheless, accumulated experience suggests at least the following considerations:

(1) Sudden changes in wind-tunnel floor elevation should be avoided between entrance and exit. Lin and Binder (1967) experienced extremely strong gravity currents due to the tendency of colder air to accelerate down contraction and diffuser sections. Segur (1969) concluded that the large contraction after the heater section in Scotti's tunnel exaggerated wave growth.

(2) Growth of boundary layers on tunnel walls will accelerate the flow and cause effective contraction; hence an adjustable side wall should be provided. Hewett *et al.* (1970) found an increase in free-stream velocity of 15% over the length of their tunnel as a result of this effect.

(3) Additional ceiling and floor thermal control should be provided to maintain a stationary thermal profile with longitudinal distance.

(4) For the low range of velocities used in the tunnel, conventional methods of



measuring velocity are unsuitable. A method should be devised which provides both wind magnitude and direction simultaneously.

The test section of the tunnel constructed has a rectangular cross-section 50 cm by 60 cm and is 460 cm long. The tunnel ceiling is adjustable to compensate for acceleration of the free stream as induced by boundary-layer growth on the walls. The ceiling can be raised a maximum of 20 cm near the end of the test section. The increase in displacement thickness for a typical flow situation is about 2.5 cm. The air flow is provided by a small four-blade fan driven by a  $\frac{1}{2}$  h.p. variable speed regulated D.C. motor. All instrument access is by means of slots cut in five removable windows. (See Figure 1 for a general view.)

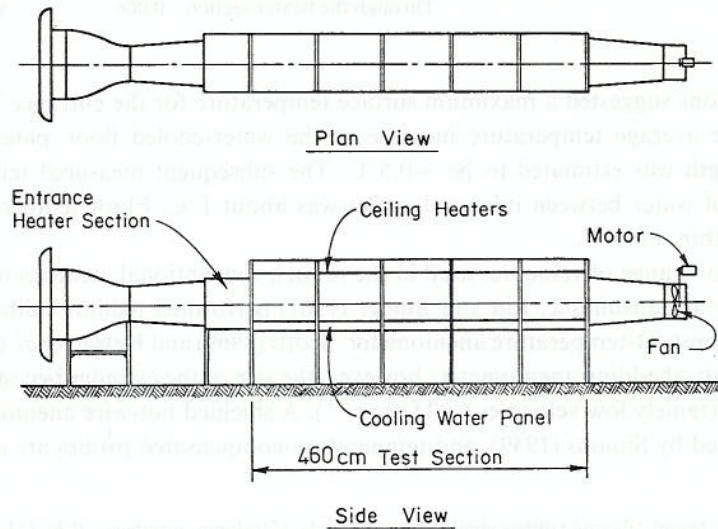
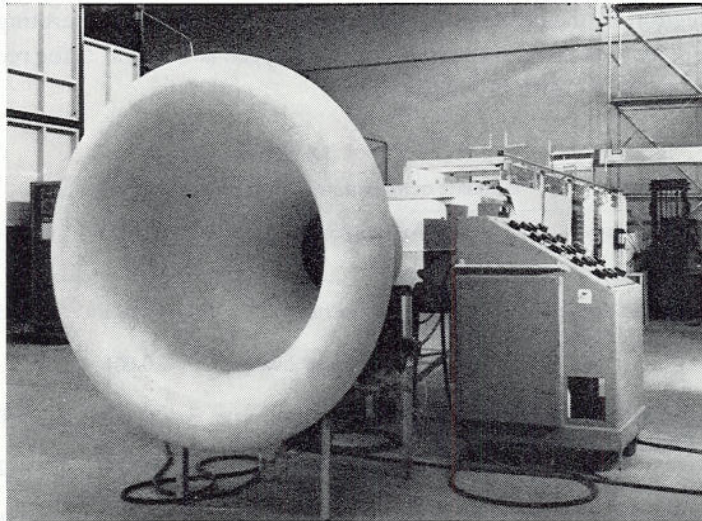


Fig. 1. General views of the stratified wind tunnel.

The stable gradient of density is created by imposing a positive vertical temperature gradient on the flow at the inlet. This is done by passing the flow through a heat exchanger constructed from sixteen flat electric sheet heaters. The heaters (15 cm  $\times$  60 cm  $\times$  0.2 cm)\* were arranged in a variably-spaced, parallel, vertical array. By adjusting the power dissipated in each heater sheet, the desired temperature profile may be created. To maintain the profiles, three larger heater pads (60 cm  $\times$  180 cm  $\times$  0.2 cm)\* were attached to the flexible tunnel ceiling with adhesive. It was necessary to provide a heat sink along the floor to maintain the thermal gradient. For this purpose, cooling panels for tap water were installed.

Simple computations were conducted to estimate the transport of energy to and from the heaters and sink. Since the room inlet conditions are known, the order of energy production by the heaters may be calculated. For a typical operating condition where ambient air is at 23°C and the desired flow speed is 15 cm s<sup>-1</sup>, the required heat exchanger behavior is shown in Table I.

TABLE I  
Estimate of maximum heat exchange performance

Heat energy	Exchanger	W cm <sup>-2</sup> (1)	Total Watts [(1) $\times$ Area]
Energy supplied to the wind tunnel	By the entrance heater	0.049	1500
	By the ceiling heater	0.001	20
Energy transferred from the wind tunnel	Through the exit	0.292	1050
	Through the floor water panel	0.010	280
	Through the side walls	0.002	100
	Through the heater section	0.006	90

Calculations suggested a maximum surface temperature for the entrance heaters of 150°C. The average temperature increase of the water-cooled floor panel over its 360-cm length was estimated to be  $\sim 0.5^\circ\text{C}$ . The subsequent measured temperature difference of water between inlet and outlet was about 1°C. Floor temperature was uniform within  $\pm 0.5^\circ\text{C}$ .

For the low range of velocities used in the tunnel, conventional methods of measuring velocity are unsuitable. Lin and Binder (1967) performed tedious calibrations to utilize the constant-temperature anemometer. Scotti (1969) and Hewett *et al.* (1970) utilized the eddy-shedding anemometer; however, the size of the cylinder becomes rather large for extremely low velocities ( $< 15 \text{ cm s}^{-1}$ ). A shielded hot-wire anemometer has been reported by Simons (1949), and temperature-compensated probes are also avail-

\* Chomalex brand silicone rubber shielded heater pads. Catalogue numbers: P/N 171-881155-002 Type SL/PSA; P/N 171-881155-001 Type SL/PSA.



able for low-speed measurements. A fairly accurate system for measuring low velocities without tedious calibration procedures and point by point measurements is the 'smoke-wire' method (Orgill *et al.*, 1971).

In the 'smoke-wire' method, oil is evaporated from a very thin, high-resistance wire by passage of a large electric current through the wire from a capacitor discharge. This forms a thin line of smoke at the wire which is carried downstream with the local velocity and deformed into the shape of a velocity profile. Calibrations indicated that heat generated at the wire might cause a 1-cm rise in the smoke trace in the worst case of very low velocities; however, over the range studied here, it was not significant. A time-delay circuit is actuated with the discharge of the capacitor which, after a predetermined time delay, simultaneously fires a strobe light and camera to illuminate

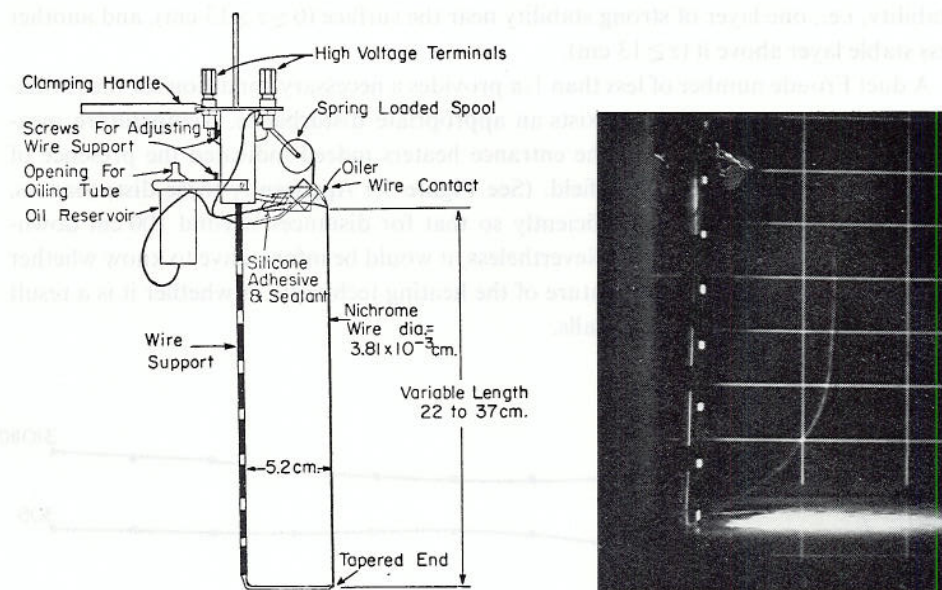


Fig. 2. Details of the smoke-wire probe used in obtaining airflow velocities and a typical velocity profile shown on a picture in a neutral case.

and photograph the smoke line. With the displacement of the smoke line measured from the film and the measured time delay, velocity profiles can be obtained. An added advantage of the system is the ability to obtain two horizontal components of velocity by utilizing two cameras and analysing paired pictures with a stereocomparator. Figure 2 shows details of the smoke-wire probe. (For further details, see Orgill *et al.* (1971). Appendix C.) Results are believed to be accurate to  $\pm 3$ –10%.

Copper-constantan thermocouples were utilized to monitor temperature variations. Sixteen thermocouples were mounted on the entrance heaters, four were on the ceiling heaters, and three were on the floor. Nine thermocouples mounted on a rake were used for vertical temperature distribution measurements – accuracy expected,  $\pm 0.5^\circ\text{C}$ .

#### 4. Operating Characteristics of the Wind Tunnel

The operating characteristics of the wind tunnel were determined using the instruments described above. Velocity profiles were measured at 200 cm downstream of the heat exchanger for mean velocities ranging from 5 to 20 cm s<sup>-1</sup>. Temperature profiles were monitored with a thermocouple rake. Smoke streamers were also released to visualize the flow condition. When the duct Froude number exceeded  $1/\pi$ , the streamlines and temperature isotherms were horizontal over the tunnel length. When the duct Froude number was less than  $1/\pi$ , horizontal streamlines and isotherms were still evident for the flow field farther than 200 cm downstream from the heater section. Isotherms in the cross-section of the tunnel were flat over 95% of the flow field, deviating slightly downward at the side walls. One common anomaly was the presence of two-layer stability, i.e., one layer of strong stability near the surface ( $0 \lesssim z \lesssim 13$  cm), and another less stable layer above it ( $z \gtrsim 13$  cm).

A duct Froude number of less than  $1/\pi$  provides a necessary condition for the formation of standing waves if there exists an appropriate disturbance. Temperature measurements just downstream of the entrance heaters indeed indicated the presence of strong disturbances in the flow field. (See Figure 3.) Apparently these disturbances, although large, are damped sufficiently so that for distances beyond 100 cm downstream, they are not significant. Nevertheless, it would be informative to know whether the disturbance is an inherent feature of the heating technique or whether it is a result of lateral heat losses to the side walls.

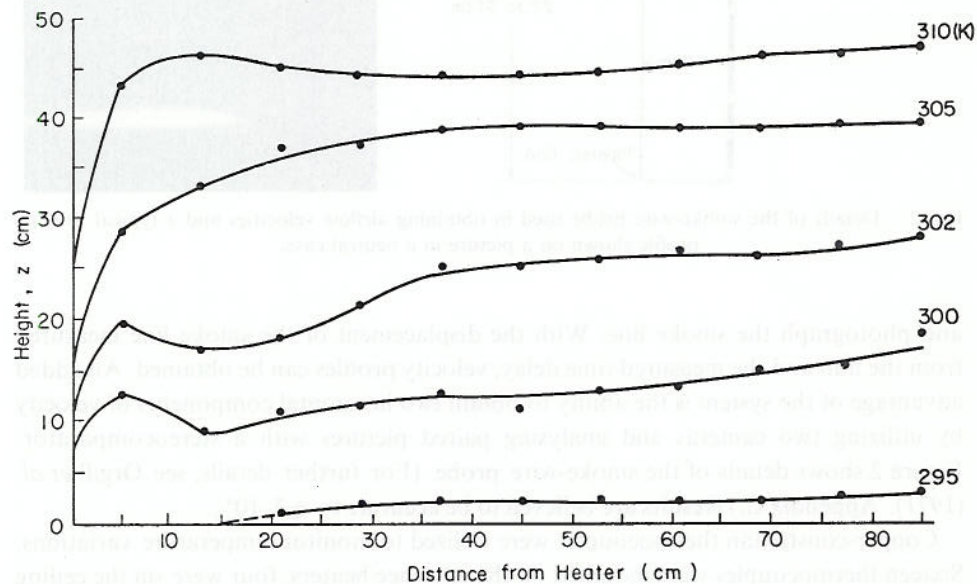


Fig. 3. Temperature contour lines downstream of the entrance heaters. Heaters were located along the vertical line at  $x = 0$ .  $Fr = 0.16$ .



### 5. Numerical Standing-Wave Experiment

A numerical computation was performed to test whether the strong disturbances were generated by the heaters at the entrance section.

The following set of Equations (1), (2), and (3), together with the definition of the stream function (4), are to be integrated numerically with appropriate boundary and initial conditions.

$$D\zeta/Dt = K\nabla^2\zeta + (g/T)(\partial T/\partial x) \quad (1)$$

$$\zeta = \nabla^2\Psi \quad (2)$$

$$DT/Dt = K'\nabla^2T \quad (3)$$

$$u = -\partial\Psi/\partial z \quad \text{and} \quad w = \partial\Psi/\partial x. \quad (4)$$

The assumptions inherent in this particular set of equations are discussed in detail by Yamada and Meroney (1971). As a result of a variety of test calculations, the boundary conditions and grid for numerical integration were specified as shown in Figure 4. The primary difficulty associated with the approximation of a partial differential equation by a finite-difference equation is due to the existence of non-linear inertial terms such as  $u\partial\zeta/\partial x$  or  $w\partial\zeta/\partial z$ . If one used a forward difference for a time derivative and a central difference for a space derivative, then the difference equation for a differential equation  $\partial\zeta/\partial t + u\partial\zeta/\partial x = 0$  is unconditionally unstable. Hence, no matter how small a time step is chosen, small errors introduced in the computation grow without limit.

A solution to this instability has been provided by a 'forward-backward' molecule

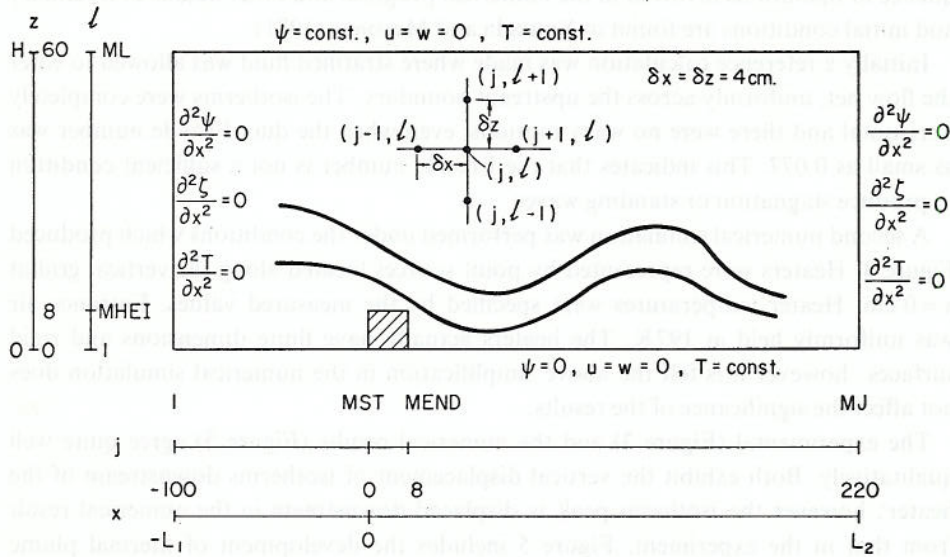


Fig. 4. Schematic diagram of the numerical region, the grid system, and boundary conditions.

which replaces convection terms by

$$\begin{aligned} \left( u \frac{\partial \zeta}{\partial x} \right)_{j,l}^n &= u_{j,l}^n \frac{\zeta_{j,l}^n - \zeta_{j-1,l}^n}{\zeta_x} \quad \text{when } u_{j,l}^n \geq 0 \\ &= u_{j,l}^n \frac{\zeta_{j+1,l}^n - \zeta_{j,l}^n}{\zeta_x} \quad \text{when } u_{j,l}^n < 0 \end{aligned}$$

This relation states that when velocity  $u_{j,l}^n$  is positive, then the space derivative is approximated by a backward difference and when it is negative, then a forward difference is used. In this way the direction of the convection is always the same as that of the local velocity components. All variables are transported from the upstream side of the point in a local sense. Subscripts  $j$  and  $l$  are  $j$ th and  $l$ th grid points in  $x$  and  $z$  directions, respectively. In the same manner, superscript  $n$  stands for  $n$ th time step of integration.  $n=1$  is an initial time.

The upstream difference scheme may introduce an 'unexpected' numerical damping which may under certain circumstances modify or control the solution for a given problem. The numerical result of this scheme is equivalent to an added diffusion effect typified by a pseudo-viscosity  $\nu_p$ . The large damping effect introduced automatically in the upstream difference system is sometimes very convenient to filter or smooth out the computational errors developed near a large temperature discontinuity. They exist in the unstably stratified regions around a model heat island which magnifies even a small error introduced during computations. These perturbations usually do not represent physically meaningful phenomena; therefore they should be numerically reduced or eliminated. Since the upstream finite-difference expression itself has a smoothing character, any computational perturbations are smoothed out. The sequence of operations involved in the numerical program and other details of boundary and initial conditions are found in Yamada and Meroney (1971).

Initially a reference calculation was made where stratified fluid was allowed to enter the flow net, uniformly across the upstream boundary. The isotherms were completely horizontal and there were no wavy motions, even when the duct Froude number was as small as 0.077. This indicates that the Froude number is not a sufficient condition to produce stagnation or standing waves.

A second numerical simulation was performed under the conditions which produced Figure 3. Heaters were represented by point sources located along the vertical grid at  $x=0$  cm. Heater temperatures were specified by the measured values. Entrance air was uniformly held at 197K. The heaters actually have finite dimensions and rigid surfaces; however it is felt the above simplification in the numerical simulation does not affect the significance of the results.

The experimental (Figure 3) and the numerical results (Figure 5) agree quite well qualitatively. Both exhibit the vertical displacement of isotherms downstream of the heater; however the isotherm peak is displaced downstream in the numerical result from that in the experiment. Figure 5 includes the development of thermal plume penetration into the upstream region from the heaters. These horizontal temperature



variations generate vorticity through the expression  $(g/T)(dT/dx)$  in the vorticity transport equation. Computed contour lines of vorticity are also included in Figure 5: a pair of large vortices are observed on both sides of the heater. A minus sign corresponds to a clockwise circulation. Streamlines are perturbed because of the intense vortices and the presence of a stagnation region.

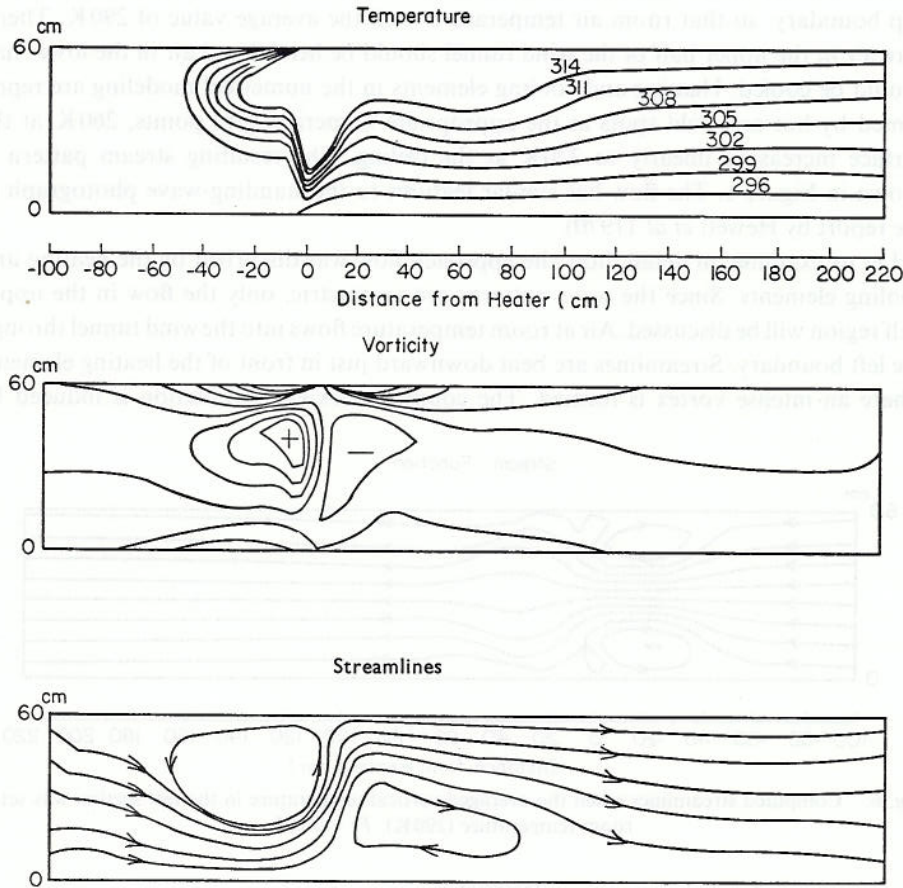


Fig. 5. Computed contour lines of temperature, vorticity, and streamlines under the same conditions as in Figure 3.

It is now clear that disturbances in the wind tunnel were created by the temperature difference between heater plates and incoming air. The disturbances thus apparently need not be due to natural convection as argued by Hewett *et al.* (1970), nor due to contraction in tunnel cross-section as suggested by Segur (1969).

In the following paragraphs, some additional numerical experiments will be discussed which seek a method to eliminate the undesirable disturbances. Hewett *et al.* (1970) maintained the average air temperature at room temperature to minimize the heat transfer through the wind-tunnel side walls. However they still observed large-

amplitude standing waves and concluded that they were caused by the natural convection of the tunnel as reviewed previously.

One can show qualitatively by utilizing a numerical program that standing waves may instead be generated by the temperature nonhomogeneity caused by the entrance heaters. For simplicity it was assumed that initial temperature distributions in the tunnel test section varied linearly from 280 K at the lower boundary to 300 K at the top boundary, so that room air temperature took the average value of 290 K. Therefore air in the upper half of the wind tunnel should be heated and air in the lower half should be cooled. Heating and cooling elements in the numerical modeling are represented by hot and cold spots at the appropriate numerical grid points, 260 K at the surface increasing linearly to 320 K at the ceiling. The resulting stream pattern is shown in Figure 6. The flow has similar features to the standing-wave photograph in the report by Hewett *et al.* (1970).

Let us examine, in detail, how the approach flow was disturbed by the heating and cooling elements. Since the wave patterns are symmetric, only the flow in the upper half region will be discussed. Air at room temperature flows into the wind tunnel through the left boundary. Streamlines are bent downward just in front of the heating elements where an intense vortex is formed. The counter-clockwise circulation is induced by

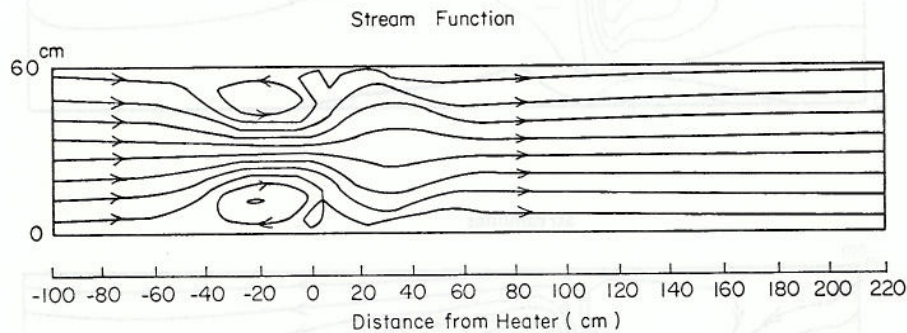


Fig. 6. Computed streamlines when the averaged vertical temperature in the test section was set at room temperature (290 K).  $Fr = 0.125$ .

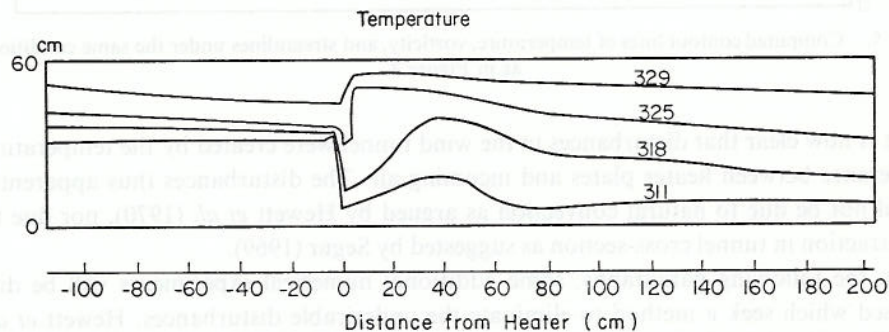


Fig. 7. Computed isotherms when the air temperature was assumed to increase linearly from room temperature to heater temperature between the upstream boundary and the heater.



upward motion of the warmer air produced by the heaters. This vortex forms a high-pressure region and blocks the airflow. Therefore the streamlines converge to the center of the tunnel where the heater has the same temperature as that of the inlet air and diverge downstream of the heaters to satisfy the continuity conditions. Since air in the tunnel is stably stratified, negative buoyant force acts to return the air particle to an equilibrium position. If an air parcel is moved beyond the equilibrium point by its inertia, then the positive buoyant force adjusts the motion. The oscillation continues until the wave energy is finally exhausted by the action of viscosity and wave interaction.

In the final numerical experiment, the incoming air temperature was increased

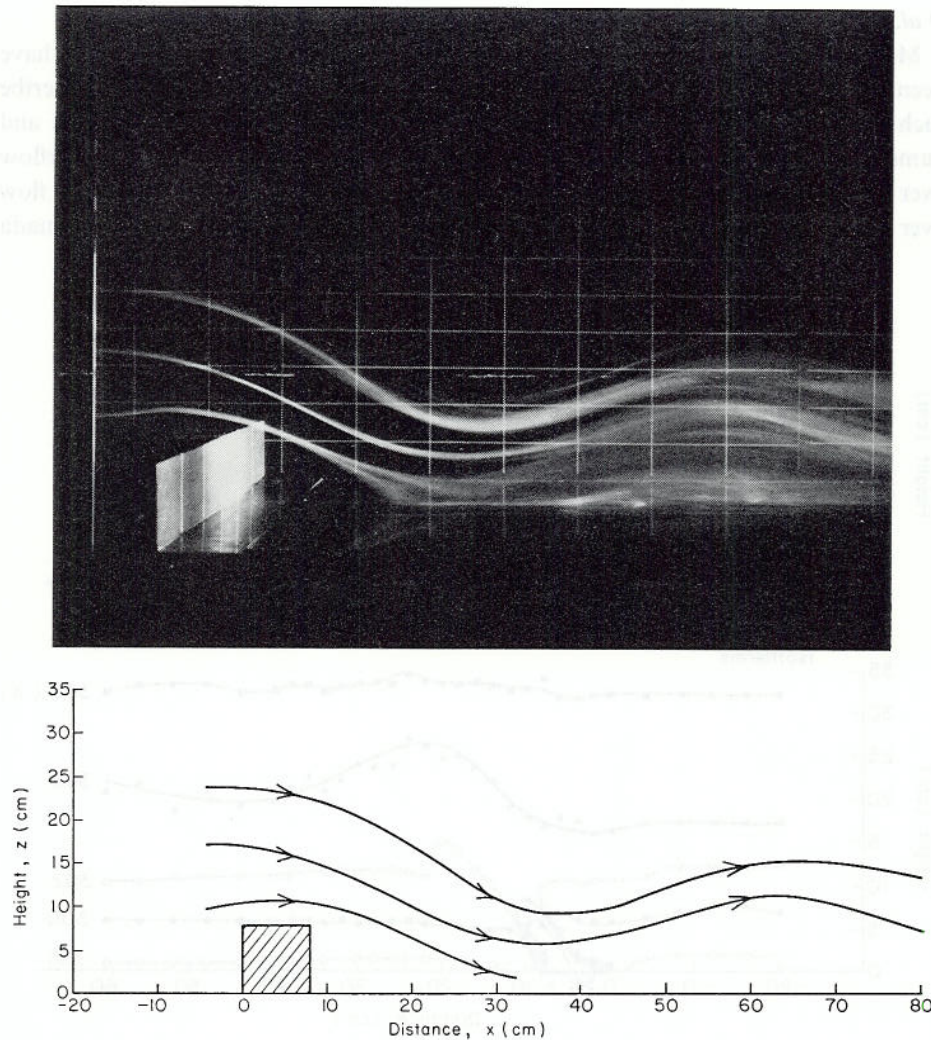


Fig. 8. Airflow over an  $8 \times 8$  cm obstacle. Streamlines obtained from a smoke visualization picture when  $Fr = 0.144$ .

linearly over a finite length. At the exit plane of the heater, its temperature was set at the same value as the desired thermal air condition. Figure 7 stubbornly exhibits the familiar large disturbances. It appears difficult to avoid or eliminate these flow perturbations even if the heat exchanger is very efficient and the exit temperature difference between heater and air is small.

Disturbances downstream of a heater in a stably stratified tunnel operated below  $Fr_D = 1/\pi$  appear un-avoidable, yet if a wind-tunnel section is long enough and waves are not strong, it is found that nearly horizontal flow will be obtained downstream as a result of the damping effects of viscosity. Indeed, even in the tunnel of Hewett *et al.* (1970), the waves are considerably diminished 100 cm downstream from the thermal control section. In the present tunnel, the length was almost double that of Hewett *et al.* (1970) and desirable flow conditions for modeling were produced.

Mountain lee-wave (internal gravity wave) and heated island disturbances have been reproduced in the present facility. It is not the intention of this paper to describe such results in detail. However, agreement between wind-tunnel measurements and numerical solutions of the equations of motion validate the laboratory flows. Airflow over obstacles (Figure 8) are reported in Yamada and Meroney (1971). Stratified flow over two-dimensional heated islands (Figure 9) is discussed by Meroney and Yamada

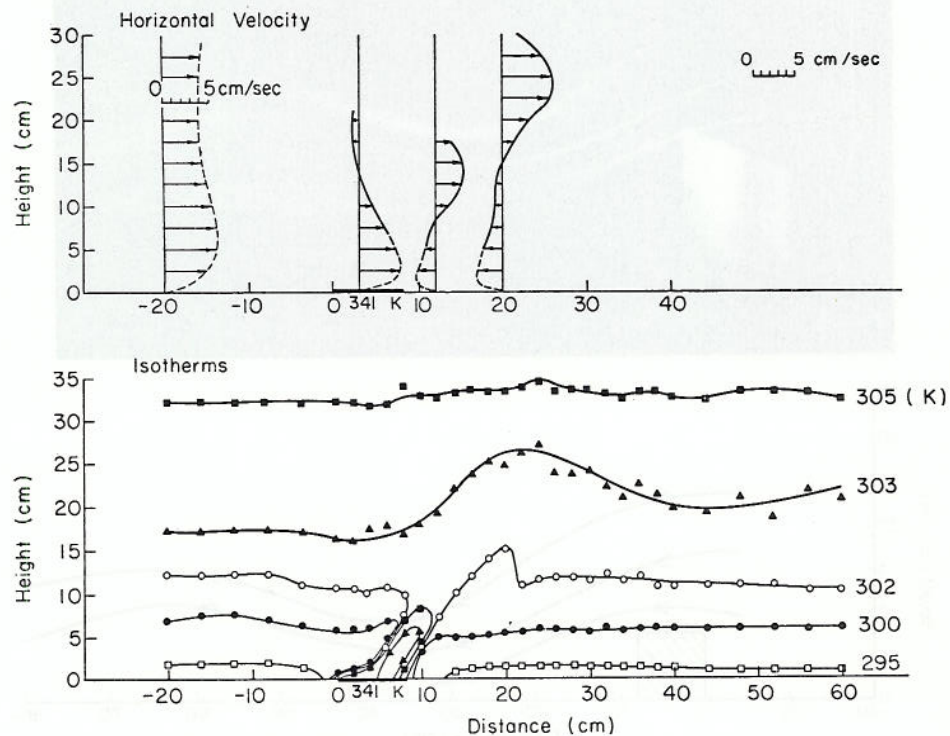


Fig. 9. Airflow over a heated island. Measured horizontal velocity profiles and isotherms when  $Fr = 0.100$ . Heat island is located from  $x = 0$  to 8 cm.



(1971). Within the accuracy of a fairly coarse computational grid, these flows were reproduced by a numerical solution of the equations of motion. Both laboratory and numerical solutions provided a valuable counterpart to linear approximation methods.

### Acknowledgements

Research Support Under THEMIS, Office of Naval Research, Contract No. N00014-68-A-0493-0001, Project No. NR062-414/6-6-68 (Code 438) is gratefully acknowledged.

### References

- Abe, M.: 1932, 'The Formation of Cloud by the Obstruction of Mount Fuji', *Geophys. Mag.*, Tokyo, 6, 1-10.
- Charpentier, C.: 1967, 'Etude de la Stabilité d'un Gradient Thermique Produit Artificiellement dans un Encoulement à Basse Vitesse au Moyer d'une Grille d'Eléments Chauffants', Département Mécanique Théorique, Electricité de France 6, Quai Watier 78 Chatou, 12 pp.
- Corcors, G. M. and Sherman, F. S.: 1970, 'Wind Tunnel Investigations of Stably-Stratified Shear Flows', presented at U.S.-Japan Seminar on Laboratory Simulation on Stratified Geophysical Shear Flows, Colorado State University, Fort Collins, Colorado, 24-26 March 1970.
- Davis, R. E.: 1969, 'Two-Dimensional Flow of a Stratified Fluid over an Obstacle', *J. Fluid Mech.* 36, 127-143.
- Hewett, T. A., Fay, J. A., and Hoult, D. P.: 1970, 'Laboratory Experiments of Smokestack Plumes in a Stable Atmosphere', Fluid Mechanics Laboratory, Department of Mechanical Engineering, Massachusetts Institute of Technology, 31 pp.
- Lin, J. T. and Binder, G. J.: 1967, 'Simulation of Mountain Lee-Waves in a Wind Tunnel', Fluid Dynamics and Diffusion Laboratory, Colorado State University, DA-AMC-28-043-65-G20, 120 pp.
- Long, R. R.: 1955, 'Some Aspects of the Flow of Stratified Fluids, III: Continuous Density Gradients', *Tellus* 7, 241-357.
- Long, R. R.: 1959, 'A Laboratory Model of Airflow over the Sierra Nevada Mountains', *The Atmosphere and the Sea in Motion*, The Rossby Memorial Volume, 372-380.
- Meroney, R. N. and Yamada, T.: 1971, 'Wind Tunnel and Numerical Experiments of Two Dimensional Stratified Airflow over a Heated Island', *Environmental and Geophysical Heat Transfer*, ASME Publication HTD-4, 31-40.
- Orgill, M. M., Cermak, J. E., and Grant, L. O.: 1971, 'Laboratory Simulation and Field Estimates of Atmospheric Transport-Dispersion over Mountainous Terrain', Fluid Dynamics and Diffusion Laboratory, Colorado State University, CER70-71MMO-JEC-LOG40, 302 pp.
- Plate, E. J. and Cermak, J. E.: 1963, 'Micrometeorological Wind Tunnel Facility, Description and Characteristics', Fluid Dynamics and Diffusion Laboratory, Colorado State University, CER63-EJP-JEC9, 39 pp.
- Pope, A. and Hooper, J. J.: 1966, *Low Speed Wind Tunnel Testing*, John Wiley and Sons.
- Queney, P. (ed.): 1960, 'The Airflow Over Mountains', World Meteorological Organization Tech. Note No. 34, 132 pp.
- Scotti, R.: 1969, 'An Experimental Study of a Stratified Shear Layer', College of Engineering, University of California, Berkeley, Rept. No. AS-69-1, 154 pp.
- Segur, H. L.: 1969, 'Stratified Flow into a Contraction', College of Engineering, University of California, Berkeley, Rept. No. AS-69-15, 178 pp.
- Simons, C. F. G.: 1949, 'A Shielded Hot-Wire Anemometer for Low Speeds', *J. Sci. Instr.* 26, 407-411.
- Stern, M. E. and Malkus, J. S.: 1953, 'The Flow of a Stable Atmosphere Over a Heated Island', Part II, *J. Meteorol.* 10, 105-120.
- Strom, G. H. and Kaplin, E. J.: 1968, 'Final Report Convective Turbulence Wind Tunnel Project', School of Engineering and Science, New York University, Rept. No. 504.04, 38 pp.
- Suzuki, S. and Yabuki, K.: 1956, 'The Airflow Crossing over the Mountain Range', *Geophys. Mag.*, Tokyo 27, 273-291.

- Webster, C. A. G.: 1964, 'An Experimental Study of Turbulence in a Density-Stratified Shear Flow', *J. Fluid Mech.* **19**, 221-245.
- Yamada, R., and Meroney, R. N.: 1971, 'Numerical and Wind Tunnel Simulation of Airflow Over an Obstacle', Presented at the National Conference on Atmospheric Waves, American Meteorological Society, Salt Lake City, Utah, October 12-15, 1971. (Also Colorado State University Civil Engineering Paper CEP70-71TY-RNM94, 37 pp.)
- Yih, C. S.: 1965, *Dynamics of Nonhomogeneous Fluids*, Macmillan, New York, 306 pp.